

MECHANISM OF LIPSS FORMATION UNDER THE INFLUENCE OF PLASMA LENS DURING FEMTOSECOND LASER PROCESSING

Sergey Dobrotvorskiy^{1,2}, Borys A. Aleksenko^{1}, Yevheniia Basova^{1*}, Iaroslav M. Gnilytskyi^{3,4},
Paweł Zawadzki⁵ and Mikołaj Kościński²*

¹National Technical University "Kharkiv Polytechnic Institute", 2, Kyrpychova str, 61002, Kharkiv, Ukraine

²Poznan University of Life Sciences, 38/42, Wojska Polskiego str, 60637, Poznań, Poland

³Lviv Polytechnic National University, 12 S. Bandery str., 79013 Lviv, Ukraine

⁴"NoviNano Lab" LLC, 5 Pasternaka, 79000 Lviv, Ukraine

⁵Adam Mickiewicz University, Uniwersytetu Poznańskiego 2, 61-614 Poznań, Poland

Emails: Borys.Aleksenko@kphi.edu.ua, Yevheniia.Basova@kphi.edu.ua

Abstract - The mechanism of formation of laser-induced periodic surface structures (LIPSS) remains unexplored and attracts the attention of researchers. We study the redistribution of laser beam energy along the path from the radiation source to the target surface, specifically in the layer of ionized ablation products formed during processing above the target surface. We take the cloud of ablation products above the target surface as a kind of lens, the material of which has a refractive index different from the refractive index of the surrounding medium. In this article, we consider the process of energy redistribution when a laser beam passes through a plasma lens formed above the target and conclude that LIPSS can be formed due to such a distribution mechanism. The process of femtosecond laser action is considered using computer modeling of the process of laser beam propagation and subsequent temperature ablation of matter from the target surface.

Keywords: Laser, Femtosecond, LIPSS, Ablation, Modelling.

1. Introduction

We assume that the formation of LIPS structures occurs due to the redistribution of the laser beam energy over the target surface. For this reason, the process occurs regardless of the properties and condition of the processed surface, its smoothness and the presence of microroughness, the homogeneity of the material, and the presence of surface oxides. We also do not consider the processes occurring inside the processed material and its surface layer. Structured deformation occurs exclusively due to the non-uniform energy impact on each specific point of the processed surface, while the non-uniformity of absorption, reflection, and the course of internal processes in the material recede into the background. In this article, we model energy redistribution along the path from the radiation source to the target surface, namely in the layer of ionized ablation products, which forms a plasma lens over the target surface.

2. Literature Review

LIPSS are periodic surface topography in two main forms, low-frequency LSFL, and high-frequency HSFL, depending on their periodicity. LIPSS is a

versatile phenomenon and can be generated on almost any material upon irradiation with linearly polarized radiation. With the advent of ultrashort laser pulses, LIPSS has become increasingly attractive over the past decade because these structures can be generated in a simple one-step process, allowing surface nanostructuring to tune the surface's optical, mechanical, and chemical properties. LSFLs, with periodicity on the order of the laser wavelength, arise from the interference of the incident light with the surface electromagnetic wave excited by the irradiation [1]. It is an open question whether LIPSS is generated by ultrafast energy deposition mechanisms acting upon the absorption of optical radiation or through self-organization following the irradiation process [2]. A two-temperature model has been developed, according to which subsequent absorption of radiation by the electron system of the irradiated material occurs, followed by the transfer of the absorbed energy to the lattice system of the solid [3 - 5] and by a multitude of subsequent thermal and possibly hydrodynamic [6, 7] or chemical effects. Due to the diversity of mechanisms and the importance of additional "feedback phenomena", a comprehensive theory of LIPSS is currently unavailable, and some aspects are still controversial and discussed in the literature. It has been studied that multi-pulse irradiation can lead to the splitting

of LSFL ridges already formed on the surface. As a result, LSFL is intermittently transformed into another LIPSS structure with half the spatial period [8, 9]. The formation of the microstructure is affected by the beam polarization direction. It has been demonstrated that for radial, azimuthal, or helical polarization of the fs laser beam, LSFL strictly follows the orientation of the local polarization direction and is directed perpendicular to it [10]. Additionally, thermocapillary and thermocapillary forces can act on the locally melted material, leading to spatial redistribution of the material during the melting process [11, 12]. LIPSSs are usually formed after irradiation with several laser pulses. Researchers [13] suggest that the first pulse creates a rough surface, facilitating energy transfer to subsequent laser pulses. Certain spatial frequencies of the roughness distribution can better absorb the radiation. Intra-pulse effects can include a short-term change in the optical properties of the solid. A wide range of composite LIPS, such as hexagonally distributed nanolattices, hexagonal nanostars, and nanorings, have been efficiently fabricated on wide bandgap semiconductors SiC and ZnO by varying the polarization combination of three beams [14, 15]. The four-beam interference method was further developed and composite LIPS such as square nanostructures, symmetric petal structures, and asymmetric helical structures were prepared on the surface of ZnO crystal. The preparation of LIPSS by three-beam interference by combining the polarization of three laser beams has been studied. [16] There are still parameters to be studied and tuned to obtain a distinct relief structure of LIPSS. One such parameter is thermal conductivity, which allows the formation of LIPSS in steel with higher regularity compared to copper, characterized by significantly higher thermal conductivity [17]. Thus, the question of the causes of the emergence of LIPSS and the conditions of their formation remains not fully understood.

3. Materials and Methods

3.1 The used Material and its Surface Microrelief

In the presented study, we use a flat plate made of AISI 321 stainless steel.

During the study, the plate was exposed to a femtosecond laser. After that, the microrelief was studied using digital microscopy, and the data obtained were compared with the results of theoretical calculations.

Theoretical calculations were performed using deform, wave, thermal, and gas-dynamic models built using COMSOL® Multiphysics software environment (RRID: RRID: SCR_014767; URL: <https://www.comsol.com/comsol-multiphysics>).

Basic materials properties were used from the built-in material properties library.

3.2 Equipment for Experiment

The state of the surface before and after treatment was examined using a Leica Emspira 3 digital microscope with a built-in LED incident illumination stand LED2000.

During the processing, optical pulses was generated by a Yb:KGW chirped pulse laser system (model PHAROS 20 W). from Light Conversions Ltd., and sent to a galvanometric scanning head (Cambridge Technology). The surface treatment was carried out in air at room temperature by scanning a laser beam over the sample's surface.

3.3 Laser Processing Simulation

We consider the propagation of a laser beam from the emission point to the target from the point of view of the laws of wave optics. We set the task of taking into account such factors that influence the intensity of ablation processes as the distribution of energy in space and the nature of its impact on the processed material. The model is based on the mechanism for calculating thermal processes and surface deformation, which we described in previous works [18]. The model is supplemented with additional calculations of the formation processes of a plasma cloud over the treated surface, which appears as a result of spallation and evaporation of particles of the processed material.

It is assumed that the speed of the femtosecond laser processing process causes intense accumulation of material in the immediate vicinity of the target (Fig. 2). This is due to the high intensity of material ablation compared to the dynamics of pressure growth in the plasma cloud. Filamentation occurs in the air before the target at a high energy density at the peak pulse power. This leads to the saturation of this region with plasma emission products and forms a film of a highly scattering vapor-droplet mixture [19 - 21]. Therefore, within the framework of the interference model, the reflection of a laser pulse normally incident on the target from the surface of a partially transparent stratum of a melted material was taken into account; the reflection of his replica, which had been passed through this stratum; the reflection from the surface of the melt underneath; as well as their resulting interference on the surface of the material [22, 23].

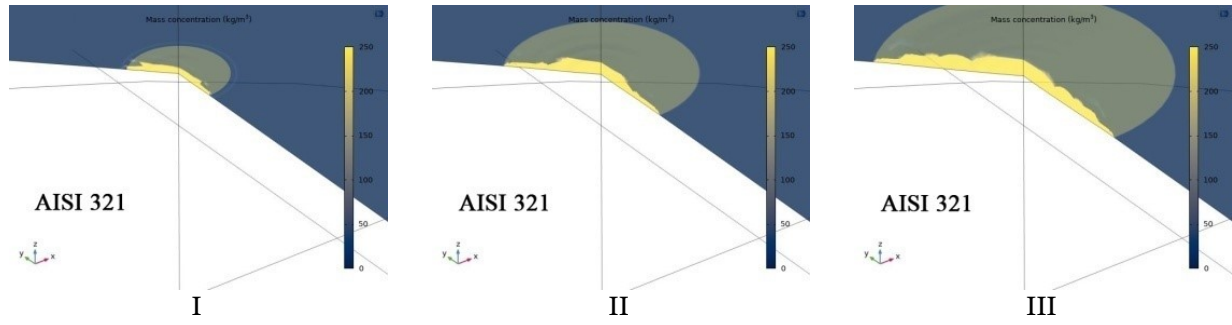


Figure 1: 3-D model, the initial growth of a plasma cloud above the target plane during material ablation

The relationship between the radius of travel of a shock wave in air and the pulse energy is related by the Sedov-Taylor dimensional relation [24]:

$$R = \lambda \left(\frac{E}{\rho} \right)^{1/(2+\beta)} t^{2/(2+\beta)}, \quad (1)$$

where λ is a constant close to 1, ρ is the initial air density, t is the expansion time, and β is the task dimension parameter, equal to 3 for spherical symmetry.

The mechanism of air saturation with temperature ablation products is described by equations for changing concentrations [25]. In this case, mass equality of the amount of evaporated material and the material forming the plasma cloud above the evaporation coordinate is assumed (Fig. 1, 3).

$$\nabla \cdot \mathbf{J}_j + \mathbf{u} \cdot \nabla c_j = R_j, \quad (2)$$

$$\mathbf{J}_j = -D_j \nabla c_j, \quad (3)$$

$$c_{\text{mass},j} = c_j M_j, \quad (4)$$

$$\omega_j = \frac{c_j M_j}{\rho_{\text{solvent}}}, \quad (5)$$

where \mathbf{J}_j is the mass flux diffusive flux vector, \mathbf{u} is the mass averaged velocity vector, c_j is the concentration of the species, R_j is a reaction rate expression for the species, D_j is the diffusion coefficient, M_j the molar mass, ω_j is the domain species volume.

Since energy transfers to the processed material by a laser beam, the computer model includes calculations of the distribution of beam energy in space. For this purpose, we use the Wave Optics module [26], which allows one to calculate the energy transfer from the emitter to the target in both homogeneous and heterogeneous media. The calculation method is intended to predict and study the propagation of electromagnetic waves and resonance effects in optical applications.

This makes it possible to analyze the distribution

of the electromagnetic field, considering transmission and reflection in the material and, accordingly, the distribution of dissipated power. Inasmuch as the refractive index in plasma is lower than in air, the beam propagation medium in the presence of a plasma cloud above the target is inhomogeneous. The vapor-droplet mixture of ablation products is a highly scattering media. Thus, the space between the outer surface of the receding away ablation cloud boundary and the target surface is filled predominantly with vapors of a substance with a refractive index $n_{\text{fi}} < 1$ [19].

Existing static models consider plasma as a passive homogeneous medium that does not change its properties when a laser pulse passes through it [27]. This approximation works in subcritical plasmas with very low densities. Collective processes occur in it on a time scale much larger than the duration of the laser pulse. The main influence exerted by the plasma on the laser pulse passing through it is mainly a local change in the refractive index, which leads to a change in its trajectory. Thus, the most correct way is to use the equations of wave optics:

$$\nabla \times \mu_r^{-1} (\nabla \times \mathbf{E}) - k_0^2 \left(\epsilon_r - \frac{j\sigma}{\omega \epsilon_0} \right) \mathbf{E} = 0 \quad (6)$$

$$E(x, y, z) = E(x, y) e^{-jk_z z} \quad (7)$$

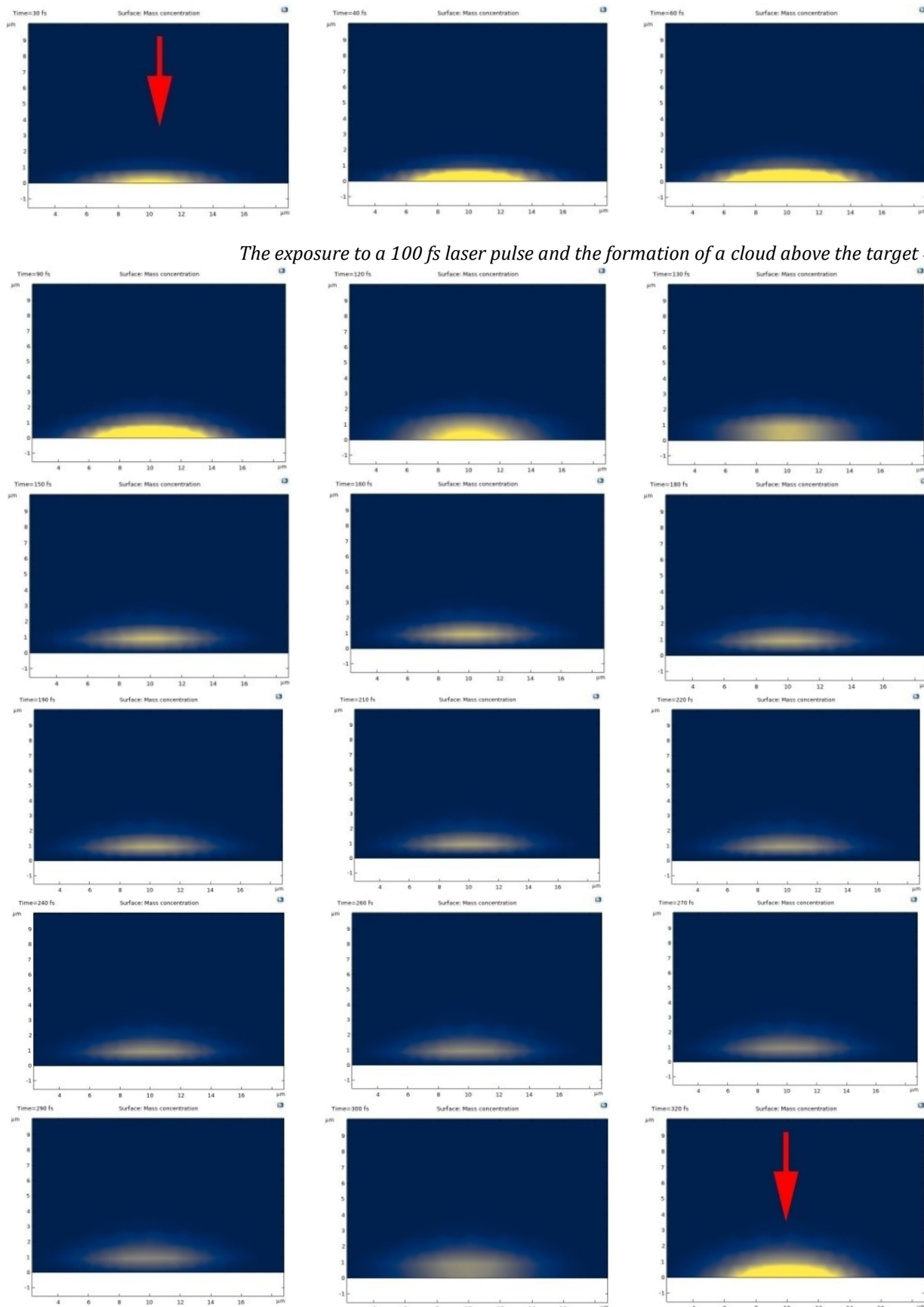
$$\nabla \times (\nabla \times \mathbf{E}) - k_0^2 \epsilon_r \mathbf{E} = 0 \quad (8)$$

$$\mathbf{n} \times (\nabla \times \mathbf{E}) - jk \mathbf{n} \times (\mathbf{E} \times \mathbf{n}) = 0 \quad (9)$$

$$E_p = \sqrt{2I_p / c \epsilon_0} \quad (10)$$

where \mathbf{E} is the electric field, ϵ_r is the relative permittivity, ϵ_0 is the permittivity of vacuum, μ_r is the relative permeability, σ is the electrical conductivity, j is the current density vector, ω is the angular frequency, k is the projection of the wave vector, \mathbf{n} is the normalized normal vector to the boundary, z is the unit vector in the z -direction.

Mechanism of LIPSS Formation under the Influence of Plasma Lens during Femtosecond Laser Processing



The exposure to a 100 fs laser pulse and the formation of a cloud above the target =>

=> Next pulse 300 fs later with the influence through the cloud

Figure 2: 2-D model, the growth of a plasma cloud above the target plane at the pulse action moment and cloud's retention in space directly above the target until the next pulse

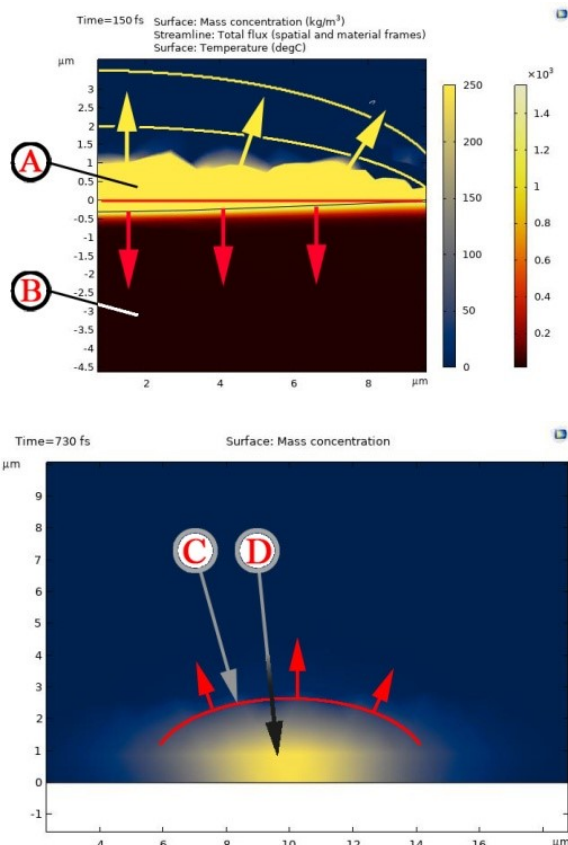


Figure 3: The mechanism of formation of a plasma cloud. A – cloud of ablation products formed above the target surface; B - material from the surface of which ablation occurs; C – the conditional transition boundary of media separation; D – the area of plasma cloud formation with a reduced scattering coefficient

Thermal processes and surface deformation are modeled similarly to what we described in previous works [18, 28]. The peak laser power in the presented models is assumed to be up to $I_p=1e17$ [W/m²] [29]. The simulation is performed with the electric field amplitude up to $E=1e10$ [V/m] (eq. 10). The initial distribution of the laser beam energy along the horizontal coordinate at the output of the laser optics is set in accordance with the Gaussian normal distribution law.

4. Results and Discussion

We have obtained calculated theoretical data on the spatial distribution of laser beam energy. Also, based on the calculations performed, the magnitude of spatial deformation of the material during its laser processing is determined from the point of view of the formation of LIPS structures

4.1 Laser Exposure through a Homogeneous Medium

Calculations show that in the case of beam propagation in a homogeneous medium (Fig. 4. I),

the energy on the target surface is distributed according to the Gaussian normal distribution law. This corresponds to the law of its distribution at the emission point (Fig. 4. II). What leads to the analogical distribution and accumulation of thermal energy inside the processed material. Deformation of the target surface also occurs according to a similar law, forming a symmetrical crater in the shape of a Gaussian cross-section. The crater is located in the center of the target, while the formation of periodic structures does not occur (Fig. 4. III).

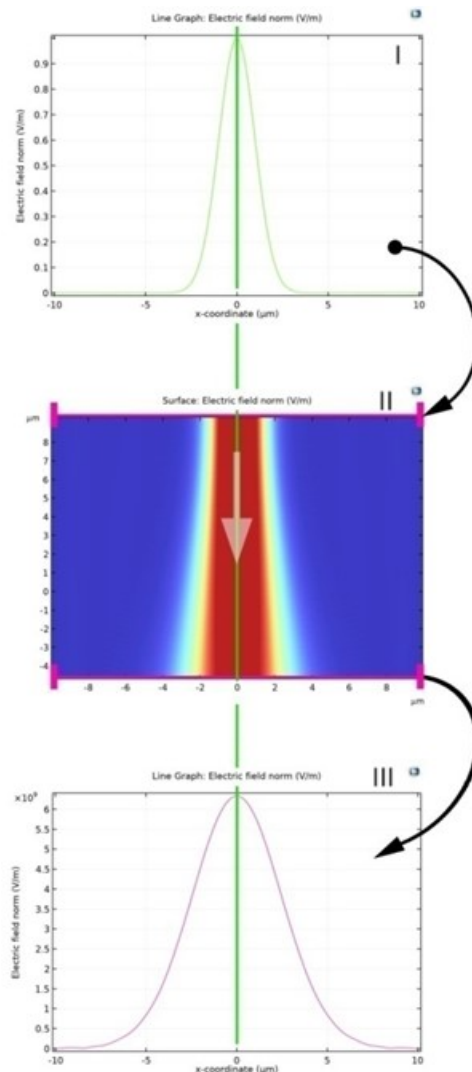


Figure 4: The scattering of a laser beam (I) and distribution of its power (III) over the surface of the target when passing through a homogeneous medium.

It should be noted that calculations performed using both a one-temperature and a two-temperature model give the same result in terms of deformation of the target surface. Also, an important requirement for building a model is sufficient saturation of the computational grid, especially when calculating the gradient of the electromagnetic field strength.

Otherwise, erroneous structural distortions may

be visualized from a random coincidence of the size of the calculation cell with the size of the resulting microstructure elements.

4.2 Laser Exposure through a Medium in which Inhomogeneity is due to the Presence of a Stationary Plasma cloud formed above the Target Surface

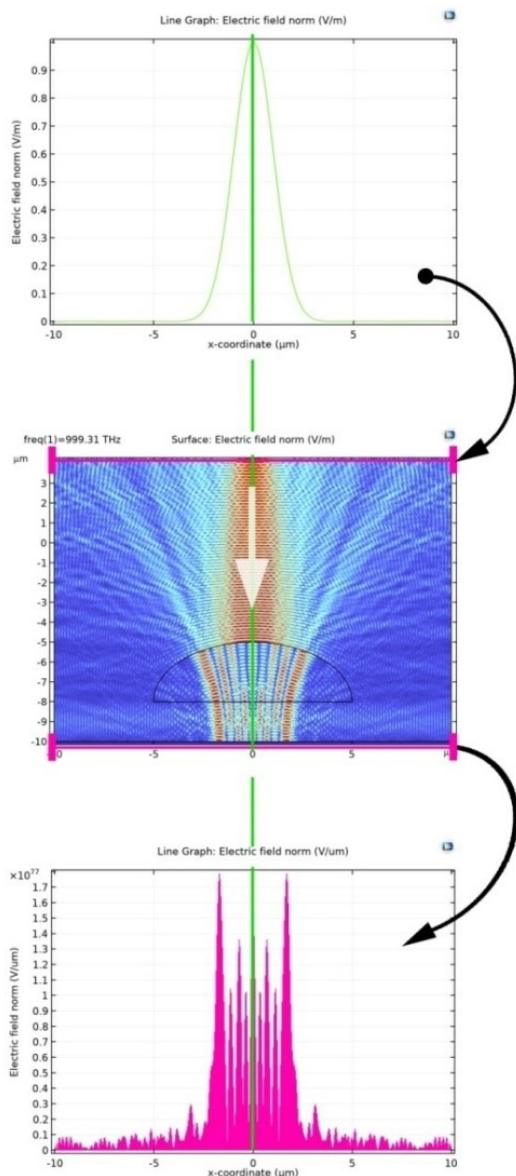
This model of forming a LIPS structure is based on the assumption that the plasma cloud formed above the target from pulse to pulse (Fig. 2) has the same spatial configuration and, thus, from the point of view of the process of energy impact on the target.

We assume that the energy transferred to the target is redistributed due to the difference in the values of the scattering coefficient in the surrounding air and the cloud of ionized ablation products.

This also occurs due to the emergence of a boundary between the media (Fig. 7. pos. B), which is theoretically modeled as a transition boundary.

When a laser beam passes through a plasma lens formed above the target surface, scattering of the beam in a heterogeneous medium is observed (Fig. 5 II). The energy on the target surface is distributed more chaotically and wave-like than at the emission point (Fig. 5. I). Thus, the distribution and accumulation of thermal energy inside the processed material also occur wave-like, forming a set of valleys on the surface of the target (Fig. 6. pos. E). The valleys create a surface microstructure with some periodicity.

The reason for the occurrence of the LIPSS effect, in this case, is exclusively the spatial redistribution of the shape-forming laser energy on the ablation products, which inevitably arise above the target surface.



I The energy distribution of the laser beam at the output of the laser optics is specified along the horizontal coordinate in accordance with the Gaussian normal distribution law.

II The scattering of laser beam energy as it passages in an inhomogeneous medium formed by a plasma cloud above the target surface.

III Laser beams energy distribution of a laser beam on the surface of a target as it passages in an inhomogeneous medium.

Figure 5: The scattering of a laser beam (I) and distribution of its power (III) over the surface of the target when passing through the inhomogeneous medium.

The described principle of microstructure formation is characterized by the fact that it does not require the expenditure of such an amount of energy, which is sufficient to create secondary force fields in the processed material and generate such wave processes that can lead to deformation of the target material with the formation of pronounced surface relief.

4.2.1. A Model of Controlled Creation of a Periodic Surface Macrostructure, which is Accompanied by the Formation of a LIPSS Structure

In the process of experimental processing of the studied sample with a femtosecond laser, a surface relief was practically obtained (Fig. 6. pos. F), with a clearly visible surface LIPSS structure (Fig. 6. pos. E) and craters (Fig. 6. pos. D) formed in the coordinates of the projection of the focus of the laser beam on the plane of the treated surface (Fig. 6. pos. A, B).

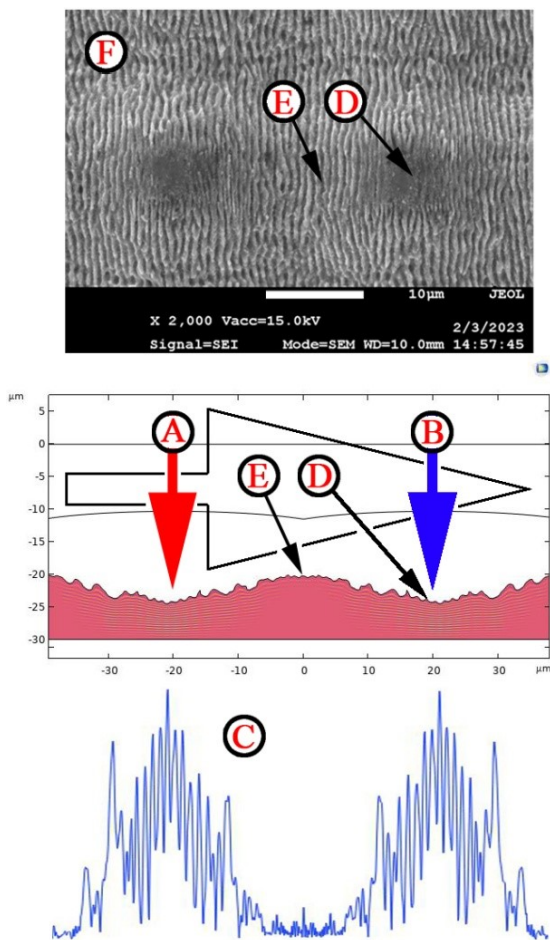


Figure 6: Formation of a periodic surface macrostructure. A, B – is the coordinates of the influence of the laser beam; C – is the energy distribution diagram over the target surface; D – is the formation of a LIPSS structure at the bottom of the crater; E – is the formation of a LIPSS structure on the surface between craters; F – the photo of the surface after processing.

Elements of the LIPSS structure are clearly visible both on the surface as a whole and on the bottom of the craters.

In this case, the surface at the bottom of the craters has a lower relief microstructure, which can be explained by the maximum energy of the laser beam in the center of the target and the melting of the material, which even continues after the cessation of active laser exposure.

We model the above deforming process assuming that a cloud of ablation products forms above each target (Fig 6. pos. A, B) and participates in the process of spatial redistribution of energy over its surface. Conditionally identical conditions and impact characteristics suggest the same redistribution mechanism for each target.

After obtaining data on the energy distribution along the plane (Fig. 6. pos. C), the surface microrelief after energy exposure was theoretically calculated. The model confirms the possibility of forming LIPSS structures both at the bottom of craters (Fig. 6. pos. E) and on the surface between them (Fig. 6. pos. D).

4.3 Laser Exposure through a Medium in which Heterogeneity is due to the Presence of a Plasma cloud increasing above the Target Surface during Laser Exposure

The mathematical model constructed for these conditions (Fig. 7) shows the dynamics of changes in the distribution of laser beam energy on the target surface caused by an increase in the size of the plasma cloud during the process of material ablation (Fig. 9).

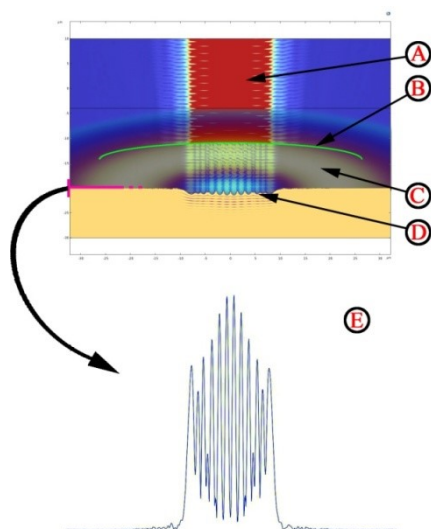


Figure 7: Laser exposure through a plasma cloud above the target surface. A – the laser beam; B – the transition boundary between media; C – the gradient of the scattering coefficient in the region of the plasma cloud; D – the surface deformation during laser ablation; E – the diagram of energy distribution over the target surface

The growth of a plasma cloud is mathematically modeled by a displacement (A => B) of the transition boundary between the air-plasma media (Fig. 10) within 6 μm with a step of 0.1 μm and a corresponding change in the gradient of the scattering coefficient's value. The laser beam scattering options that arise during this modification of the plasma lens form the corresponding patterns of intensity distribution on the target surface. From the summary diagram (Fig. 10. pos. C), reflecting the nature of changes in the energy distribution, we can conclude that in order to create the conditions for the formation of a clearly defined LIPS structure, it is necessary to invariably

maintain shape and size of the plasma cloud within the limits of at least 0.1 microns throughout the entire period of energy exposure. Otherwise, the cumulative effect leads to a total energy impact, the surface distribution of which approaches normal (Fig. 10. pos. C) with the formation of a crater with the corresponding cross-sectional shape.

Since it is impossible to create the appropriate conditions (Fig. 5, 7, 8) in practice, it should be concluded that the formation of LIPS structures is impossible due to the redistribution of the energy of the laser beam when propagating through the plasma lens.

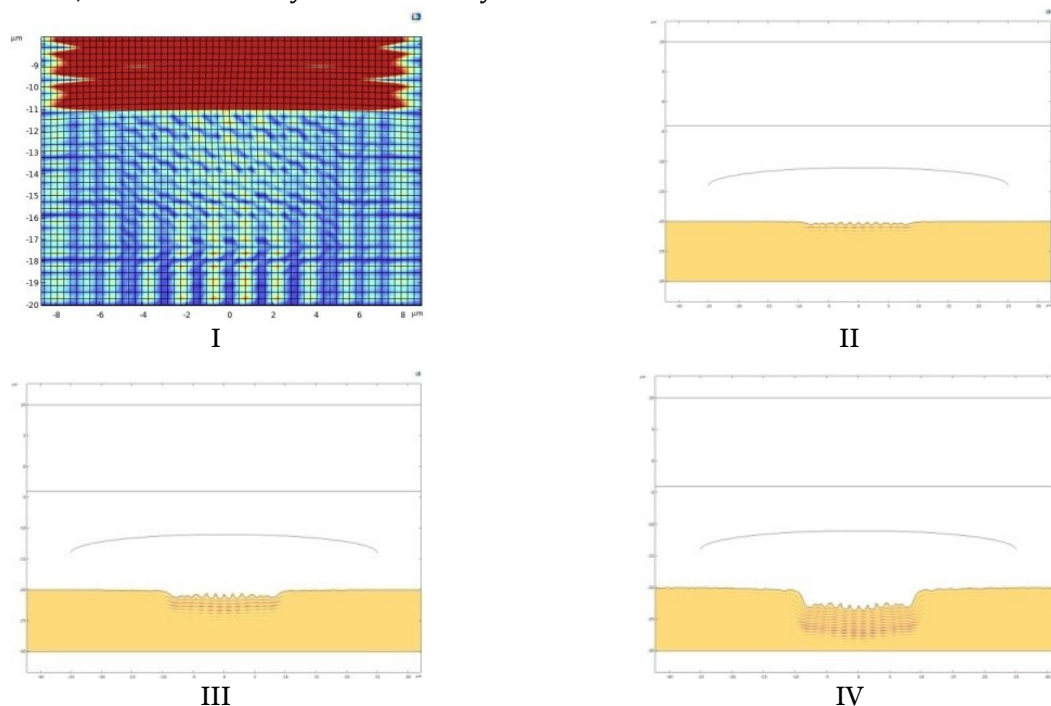


Figure 8: I – The calculation mesh of the model; II-IV – is the dynamics of the target surface deformation in the case of constant dimensions of the plasma cloud and its standing location above the target surface.

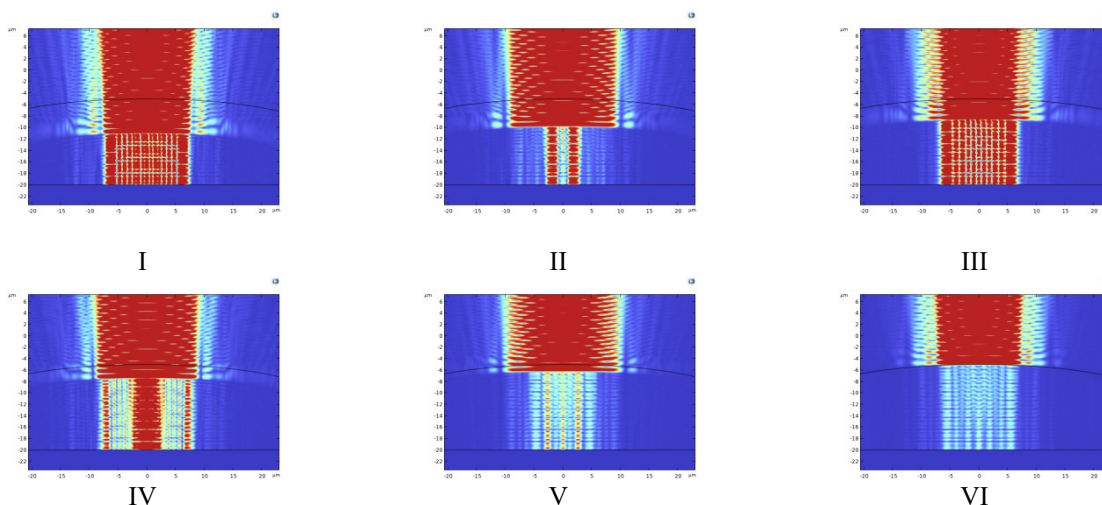


Figure 9: The growth of a plasma cloud above the target plane at the pulse action moment and the cloud's retention in space directly above the target until the next pulse.

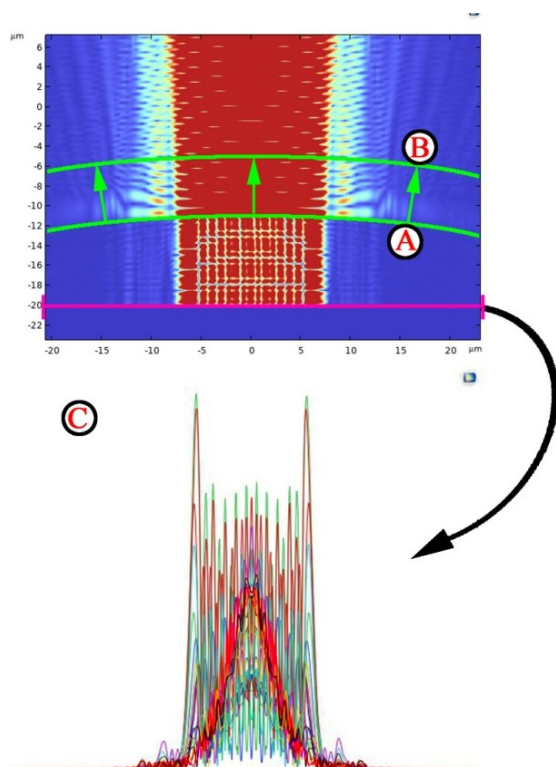


Figure 10: Laser exposure through a plasma cloud growing above the target surface. A - B – is the displacement of the interface between media during cloud growth; C – the diagrams of energy distribution over the target surface at different positions of the transition boundary between the medias

It also makes no sense to construct a theory that explains the directional nature of the LIPSS structure formed by this method.

5. Conclusions

The study's results allow us to state the influence of the plasma cloud on the scattering of the laser beam and, consequently, on the formation of the microrelief obtained by laser irradiation. It was found that a homogeneous plasma cloud, acting as a plasma lens, can cause an uneven distribution of the laser beam power over the target surface but does not ensure a stable process of obtaining LIPSS. The variants of laser beam scattering that arise during the spatial modification of the plasma lens form different energy distribution patterns on the target surface. To create conditions for the formation of a clearly defined LIPSS with a period comparable to the wavelength, it is necessary to consistently maintain the shape and size of the plasma cloud, preventing its deformations and displacements within 10% of the wavelength, or about 0.1 μm , throughout the entire period of energy exposure. Otherwise, the cumulative effect leads to a total energy impact, which surface distribution approaches the normal one.

In this case, a crater is formed, the cross-sectional shape of which is close to a Gaussian. Since it is impossible to create the corresponding conditions in practice, it should be concluded that LIPSS formation due to the plasma lens effect causes difficulties. Furthermore, beam scattering by the plasma lens does not provide a comprehensive explanation for the reason for the current directed nature of the LIPSS structure.

Our theory of the formation of a stable spatial periodic structure in a plasma cloud based on the principle of Rayleigh waves, which determines a stable periodic distribution of laser beam energy over the target surface in the direction of beam polarization, is undergoing practical testing. Also in the future is a study of the influence of an additional magnetic field on the change in the character of LIPSS

Acknowledgments

The general approach was developed within the research project "Formation and transformation of periodic nanocarbon-containing structures on metal surfaces with short-pulse laser, microwave, and plasma methods" (No. 0124U000481) supported by the Ministry of Education and Science of Ukraine. The authors also acknowledge the nLab, represented by Dr. Aleksander Biegunski, the FLUENCE technology, represented by Dr. Bogusz Stepak and Mrs. Natalia Grudzien, and the Renishaw firm.

References

- [1] Gnilitskyi, I., Derrien, T.J.-Y., Levy, Y., Bulgakova, N.M., Mocek, T. and Orazi, L. (2017). High-speed manufacturing of highly regular femtosecond laser-induced periodic surface structures: physical origin of regularity. *Scientific Reports*, 7(1). <https://doi.org/10.1038/s41598-017-08788-z>
- [2] Bonse, J., Höhm, S., Kirner, S.V., Rosenfeld, A. and Krüger, J. (2017). Laser-Induced Periodic Surface Structures— A Scientific Evergreen. *IEEE Journal of Selected Topics in Quantum Electronics*, [online] 23(3). <https://doi.org/10.1109/JSTQE.2016.2614183>
- [3] E. Leveugle and L.V. Zhigilei (2004). Microscopic mechanisms of short pulse laser spallation of molecular solids. *Applied physics. A, Materials science & processing*, 79(4-6), pp.753–756. <https://doi.org/10.1007/s00339-004-2609-y>.
- [4] Wu, C. and Zhigilei, L.V. (2013). Microscopic mechanisms of laser spallation and ablation of metal targets from large-scale molecular dynamics simulations. *Applied Physics A*, 114(1), pp.11–32. <https://doi.org/10.1007/s00339-013-8086-4>.
- [5] Zhigilei, L.V., Lin, Z. and Ivanov, D.S. (2009). *Atomistic Modeling of Short Pulse Laser Ablation*

- of Metals: Connections between Melting, Spallation, and Phase Explosion. The Journal of Physical Chemistry C, 113(27), pp.11892–11906. <https://doi.org/10.1021/jp902294m>.
- [6] Kozhushko, A. (2023). Hydrodynamics analysis on partially filled agricultural tanks by driving cycle of transportation, International Conference on Reliable Systems Engineering (ICoRSE), 762. https://doi.org/10.1007/978-3-031-40628-7_21
- [7] Kozhushko, A., Pelypenko, Y., Kravchenko, S., Danylenko, V. (2023). Improving the Procedure for Modeling Low Frequency Oscillations of the Free Surface Liquid in a Tractor Tank. Eastern-European Journal of Enterprise Technologies, 122 (7), pp. 61-68. <https://doi.org/10.15587/1729-4061.2023.277254>
- [8] Huang, M., Cheng, Y., Zhao, F. and Xu, Z. (2012). The significant role of plasmonic effects in femtosecond laser-induced grating fabrication on the nanoscale. Annalen der Physik, 525(1-2), pp.74–86. <https://doi.org/10.1002/andp.201200136>.
- [9] Hou, S., Huo, Y., Xiong, P., Zhang, Y., Zhang, S., Jia, T., Sun, Z., Qiu, J. and Xu, Z. (2011). Formation of long- and short-periodic nanoripples on stainless steel irradiated by femtosecond laser pulses. Journal of Physics D: Applied Physics, 44(50), p.505401. <https://doi.org/10.1088/0022-3727/44/50/505401>.
- [10] JJ Nivas, J., He, S., Rubano, A., Vecchione, A., Paparo, D., Marrucci, L., Bruzzese, R. and Amoroso, S. (2015). Direct Femtosecond Laser Surface Structuring with Optical Vortex Beams Generated by a q-plate. Scientific Reports, 5(1). <https://doi.org/10.1038/srep17929>.
- [11] E. Haro-Poniatowski, C. Acosta-Zepeda, G. Mecalco, Hernández-Pozos, J.L., N. Batina, I. Morales-Reyes and Bonse, J. (2014). Diffraction-assisted micropatterning of silicon surfaces by ns-laser irradiation. Journal of Applied Physics, 115(22). <https://doi.org/10.1063/1.4882660>.
- [12] D. Bäuerle, Laser Processing and Chemistry, Berlin, Germany: Springer-Verlag, 2011. <https://doi.org/10.1007/978-3-642-17613-5>.
- [13] Golosov, E.V., Ionin, A.A., Kolobov, Y.R., Kudryashov, S.I., Ligachev, A.E., Makarov, S.V., Novoselov, Y.N., Seleznev, L.V., Sinitsyn, D.V. and Sharipov, A.R. (2011). Near-threshold femtosecond laser fabrication of one-dimensional subwavelength nanogratings on a graphite surface. Physical Review B, 83(11). <https://doi.org/10.1103/physrevb.83.115426>.
- [14] Xiong, P., Jia, T., Jia, X., Feng, D., Zhang, S., Ding, L., Sun, Z., Qiu, J. and Xu, Z. (2011). Ultraviolet luminescence enhancement of ZnO two-dimensional periodic nanostructures fabricated by the interference of three femtosecond laser beams. New Journal of Physics, 13(2), p.023044. <https://doi.org/10.1088/1367-2630/13/2/023044>.
- [15] Jia, X., Jia, T.Q., Ding, L.E., Xiong, P.X., Deng, L., Sun, Z.R., Wang, Z.G., Qiu, J.R. and Xu, Z.Z. (2009). Complex periodic micro/nanostructures on 6H-SiC crystal induced by the interference of three femtosecond laser beams. Optics Letters, 34(6), pp.788–788. <https://doi.org/10.1364/ol.34.000788>.
- [16] Zhang, Y., Jiang, Q., Long, M., Han, R., Cao, K., Zhang, S., Feng, D., Jia, T., Sun, Z., Qiu, J. and Xu, H. (2022). Femtosecond laser-induced periodic structures: mechanisms, techniques, and applications. Opto-Electronic Science, 1(6), pp.220005–220005. <https://doi.org/10.29026/oes.2022.220005>.
- [17] Tauras Bukelis, Eugenijus Gaižauskas, Balachninaite, O. and Domas Paipulas (2023). Femtosecond IR and UV laser induced periodic structures on steel and copper surfaces. Surfaces and Interfaces, 38, pp.102869–102869. <https://doi.org/10.1016/j.surfin.2023.102869>.
- [18] Sergey Dobrotvorskiy, Aleksenko, B.A., Mikołaj Kościński, Yevheniia Basova and Vadym Prykhodko (2023). Modeling and Surface Modification of AISI 321 Stainless Steel by Nanosecond Laser Radiation. *Lecture notes in mechanical engineering*, pp.205–215. https://doi.org/10.1007/978-3-031-32767-4_20.
- [19] Kudryashov S. I. (2019). Vzaimodeystviye femtosekundnykh lazernykh impul'sov v rezhime ablyatsii s metallami i poluprovodnikami, obladayushchimi sil'nym mezhzonnym pogloshcheniyem. [Interaction of femtosecond laser pulses in ablation mode with metals and semiconductors with strong interzone absorption.] *disserCat*. [in Russian] Available at: <https://www.dissercat.com/content/vzaimodeis-tvie-femtosekundnykh-lazernykh-impulsov-v-rezhime-ablyatsii-s-metallami-i-poluprov> [Accessed 20 Feb. 2023].
- [20] K. Sokolowski-Tinten, Bialkowski, J., M. Boing, A. Cavalleri and von (1998). Thermal and nonthermal melting of gallium arsenide after femtosecond laser excitation. *Physical review. B, Condensed matter*, 58(18), pp.R11805–R11808. <https://doi.org/10.1103/physrevb.58.r11805>.
- [21] K. Sokolowski-Tinten, J. Białkowski, A. Cavalleri, M. Boing, Schueler, H. and von (1998). Dynamics of femtosecond-laser-induced ablation from solid surfaces. *Proceedings of SPIE*. <https://doi.org/10.1117/12.321593>.
- [22] K. Sokolowski-Tinten, Bialkowski, J., A. Cavalleri, von, Oparin, A.M., J. Meyer-ter-Vehn and Anisimov, S.I. (1998). Transient States of Matter during Short Pulse Laser Ablation. 81(1), pp.224–227. <https://doi.org/10.1103/physrevlett.81.224>.

- [23] von der Linde, D., Sokolowski-Tinten, K. and Bialkowski, J. (1997). Laser–solid interaction in the femtosecond time regime. *Applied Surface Science*, 109-110, pp.1–10. [https://doi.org/10.1016/s0169-4332\(96\)00611-3](https://doi.org/10.1016/s0169-4332(96)00611-3).
- [24] Zeldovich, Ya.B., Raiser, Yu.P. (1966). *Fizika udarnykh voln i vysokotemperaturnykh gidrodinamicheskikh yavleniy* [Physics of shock waves and high-temperature hydrodynamic phenomena]. Moscow: Nauka, [in Russian]. p.944. ISBN 048613508X, 9780486135083.
- [25] COMSOL Multiphysics. Chemical Reaction Engineering Module User's Guide. (2022). Available at: <https://doc.comsol.com/6.2/docserver/#!/com>. [Accessed 20 Feb. 2023].
- [26] COMSOL Multiphysics. Ray Optics Module User's Guide. (2022). Available at: <https://doc.comsol.com/6.1/doc/com.comsol.help.roptics/RayOpticsModuleUsersGuide.pdf> [Accessed 20 Feb. 2023].
- [27] Sedov M. V. (2020) *Modelirovaniye kharakteristicheskogo rentgenovskogo izlucheniya femtosekundnoy lazernoy plazmy* [Simulation of characteristic X-rays of femtosecond laser plasma]. disserCat. Saint Petersburg [in Russian]. Available at: <https://www.dissercat.com/content/modelirovaniye-kharakteristicheskogo-rentgenovskogo-izlucheniya-femtosekundnoi-lazernoi-plazm>. [Accessed 22 Feb. 2023].
- [28] Sergey Dobrotvorskiy, Yevheniia Basova, Ludmila Dobrovolska, Popov, V. and Samra, A. (2022). Creation of a Superhydrophilic Surface with Anti-icing Properties for X18H10T Stainless Steel Using a Nanosecond Laser. *Lecture notes in networks and systems*, pp.172–184. doi:https://doi.org/10.1007/978-3-031-15944-2_17.
- [29] Petrov, G.M., Davidson, A., Gordon, D., B. Hafizi and J. Peñano (2021). Thermionic emission of electrons from metal surfaces in the warm dense matter regime. *Physics of plasmas*, [online] 28(8). doi:<https://doi.org/10.1063/5.0054955>.